Research Square

Preprints are preliminary reports that have not undergone peer review.
They should not be considered conclusive, used to inform clinical practice,
or referenced by the media as validated information.

Performance Evaluation of HFO/Ionic-Liquid Working Pairs for Single-Effect and Compression-Assisted Absorption Refrigeration Cycles

Yao Zhang

zhangyao@haue.edu.cn

Henan University of Engineering

Shu Jiang

Henan University of Engineering

Article

Keywords: absorption refrigeration, hydrofluoroolefin, ionic liquid, compression-assisted cycle

Posted Date: July 31st, 2026

DOI: https://doi.org/10.21203/rs.3.rs-10307466/v1

License: This work is licensed under a Creative Commons Attribution 4.0 International License.
Read Full License

Additional Declarations: No competing interests reported.

Version of Record: A version of this preprint was published at Scientific Reports on September 18th, 2026. See the published version at https://doi.org/10.1038/s41598-026-71896-2.

Performance Evaluation of HFO/Ionic-Liquid Working Pairs for Single-Effect and Compression-Assisted Absorption Refrigeration Cycles

Yao zhang, Shu Jiang

Henan University of Engineering, Zhengzhou 451191, Henan, China

Corresponding author: Yao zhang

Correspondence: zhangyao@haue.edu.cn

Abstract: This study evaluates the application potential of four low-GWP HFO/ionic-liquid working pairs in absorption refrigeration systems. The NRTL activity coefficient model was used to describe the vapor-liquid equilibrium behavior of the working pairs, and thermodynamic models of single-effect and compression-assisted absorption cycles were established. The effects of generation, absorption, condensation, and evaporation temperatures on circulation ratio, solution concentration difference, COP, and exergy efficiency were analyzed. Results show that higher generation and evaporation temperatures improve cycle performance, while higher absorption and condensation temperatures reduce it. Among the investigated pairs, R1234ze(E)/[C4mim][DCA] exhibits the best overall performance. The compression-assisted cycle further enlarges the operating range and reduces the circulation ratio, showing good potential for low-grade heat-driven refrigeration.

Keywords: absorption refrigeration; hydrofluoroolefin; ionic liquid; compression-assisted cycle

1 Introduction

Low-global-warming-potential working pairs are essential for the development of absorption refrigeration systems driven by low-grade thermal energy, such as industrial waste heat, solar thermal energy and other renewable heat sources[1,2]. Ionic liquids have been widely considered as alternative absorbents because of their negligible vapor pressure, good thermal stability and tunable molecular structures, while hydrofluoroolefin refrigerants provide environmentally favorable refrigerant candidates for next-generation refrigeration and heat-pump systems[2,3].

In this work, four hydrofluoroolefin/ionic-liquid working pairs, namely R1234yf/[C_2mim][DCA], R1234yf/[C_4mim][DCA], R1234ze(E)/[C_2mim][DCA] and R1234ze(E)/[C_4mim][DCA], were investigated for single-effect and compression-assisted absorption refrigeration cycles. The vapor–liquid equilibrium behavior of the refrigerant/ionic-liquid mixtures was described using an NRTL-based thermodynamic model, and the required binary interaction parameters were taken from literature data for R1234yf and R1234ze(E) in dicyanamide-based ionic liquids[4,5]. A cycle model was then established based on mass and energy balance equations to evaluate the circulation ratio, solution

concentration difference, coefficient of performance and exergy efficiency under different operating conditions.

The previous studies indicate that the cycle performance of working pairs is strongly affected by both phase-equilibrium characteristics and operating temperatures. Increasing the generator temperature and evaporator temperature is favorable for enlarging the concentration difference between the strong and weak solutions, thereby reducing the solution circulation ratio and improving the thermodynamic performance of the system. In contrast, higher condenser and absorber temperatures weaken refrigerant absorption/desorption behavior and lead to performance degradation. Comparative analysis shows that the refrigerant type and the alkyd-chain length of the ionic-liquid cation significantly influence the absorption capacity, circulation requirement and cycle efficiency of the working pairs[6,7]. For the compression-assisted configuration, increasing the absorption pressure can enhance the absorption driving force, reduce the required solution circulation rate and extend the operating adaptability of the cycle under low-grade heat-source conditions[8-9]. This study provides a theoretical basis for screening environmentally friendly with working pairs and optimizing ionic absorption refrigeration systems.

2. Correlation of Solubility for HFO/Ionic Liquid Working Pairs

In absorption refrigeration cycles, vapor-liquid equilibrium (VLE) behavior directly determines the solubility of the refrigerant in the ionic-liquid absorbent and governs the absorption/desorption capability of the working pair. It also affects the concentration difference between the strong and weak solutions, which is a key parameter for calculating the circulation ratio and evaluating cycle performance. Therefore, accurate correlation of the VLE properties is essential for the thermodynamic analysis of HFO/[DCA] working pairs. In this study, the non-random two-liquid (NRTL) activity-coefficient model was adopted to describe the liquid-phase and to correlate the phase-equilibrium behavior of R1234yf/[C_2mim][DCA], R1234yf/[C_4mim][DCA], R1234ze(E)/[C_2mim][DCA] and R1234ze(E)/[C_4mim][DCA]. The governing equations of the NRTL model are expressed as Eqs.(1) and (2)

$$\ln \gamma_1 = x_2^2 \left[\tau_{21} \left(\frac{\exp(-\alpha\tau_{21})}{x_1 + x_2 \exp(-\alpha\tau_{21})} \right)^2 + \frac{\tau_{12} \exp(-\alpha\tau_{12})}{[x_2 + x_1 \exp(-\alpha\tau_{12})]^2} \right] \quad (1)$$

$$\ln \gamma_2 = x_1^2 \left[\tau_{12} \left(\frac{\exp(-\alpha\tau_{12})}{x_2 + x_1 \exp(-\alpha\tau_{12})} \right)^2 + \frac{\tau_{21} \exp(-\alpha\tau_{21})}{[x_1 + x_2 \exp(-\alpha\tau_{21})]^2} \right] \quad (2)$$

In Eqs. (1) and (2), τ_{12} and τ_{21} are the binary interaction parameters of the NRTL model[10], and α is the non-randomness parameter. To account for the temperature dependence of the liquid-phase interaction between the refrigerant and ionic liquid, τ_{12} and τ_{21} were expressed as functions of temperature, as given in Eq. (3).

$$\tau_{12} = \tau_{12}^{0} + \frac{\tau_{12}^{1}}{T} \qquad \tau_{21} = \tau_{21}^{0} + \frac{\tau_{21}^{1}}{T} \tag{3}$$

The adjustable parameters in Eq. (3) were obtained by regressing the experimental vapor-liquid equilibrium data of the corresponding cycle systems reported in the literature[11-12]. In the present work, component 1 denotes the HFO refrigerant, namely R1234yf or R1234ze(E), and component 2 denotes the ionic liquid, namely [C_2mim][DCA] or [C_4mim][DCA].The activity coefficient$\gamma_i$calculated from the NRTL model was then introduced into the phase-equilibrium equation. For the binary refrigerant/ionic-liquid mixture, the equilibrium relationship can be written as Eq. (4).

$$y_i p\phi_i = x_i \gamma_i p_i^s \quad (i=1,\ 2) \tag{4}$$

In Eq. (4), x_i and y_i represent the mole fractions of component i in the liquid and vapor phases, respectively. The equilibrium pressure is denoted by p, and the saturated vapor pressure of the pure component is denoted by p_i^s. The vapor-phase fugacity coefficient is represented by ϕ_i and was calculated using Eq (5). Because ionic liquids have extremely low vapor pressures under the investigated operating conditions, the vapor phase was assumed to be dominated by the refrigerant component. This treatment is commonly adopted in the thermodynamic modeling of refrigerant/ionic-liquid working pairs.

$$\phi_i = \exp[\frac{(B_i - V_i)(p - P_i^s)}{RT}] \tag{5}$$

Table. 1 Binary Interaction Parameters of Working Pairs by Fitting the Experimental Solubility Data[13]

Working pairs	α	$\tau_{12,0}$	$\tau_{12,1}$	$\tau_{21,0}$	$\tau_{21,1}$
R1234yf/[C_2mim][DCA]	0.2	4.893	399.13	4.4	-843.39
R1234yf//[C_4mim][DCA]	0.2	10.127	-906.24	3.420	- 671.41
R1234ze(E)/[C_2mim][DCA]	0.2	0.0081	2848.5	0.003	286.69
R1234ze(E)/[C_4mim][DCA]	0.2	0.0079	3136.7	0.002	206.22

For the absorption refrigeration cycle calculation, the thermodynamic properties of the refrigerant/ionic-liquid solution are required. The specific enthalpy of the mixture was calculated by considering the contributions of the pure refrigerant, the pure ionic liquid and the excess enthalpy caused by liquid-phase non-ideality, as expressed in Eq. (6)

$$H = x_1 H_1 + x_2 H_2 + H^E \tag{6}$$

In this equation, h1 and h2 are the specific enthalpies of the refrigerant and ionic liquid, respectively, while H^E represents the excess enthalpy of the mixture.

$$H_2 = \int_{T_0}^{T} c_{p,IL} dT + \int_{p_0}^{p} v_{IL} dp + H_0 \tag{7}$$

$$H^E = -RT^2 \sum_{i=1}^{2} x (\frac{\partial \ln \gamma_i}{\partial T})_{p,x} \tag{8}$$

The excess enthalpy was obtained from the temperature dependence of the excess Gibbs free energy derived from the NRTL model, as shown in Eqs. (7) and (8). This treatment enables the

influence of non-ideal molecular interactions between the HFO refrigerant and the ionic-liquid absorbent to be included in the cycle energy analysis. The thermodynamic properties of the ionic liquid were evaluated using temperature-dependent correlations for the isobaric molar heat capacity and molar volume, as given in Eqs. (9) and (10). In these equations, $c_{p,IL}$ is the isobaric molar heat capacity of the ionic liquid, v_{IL} is the molar volume, and R is the universal gas constant[14,15].

$$c_{p,IL} = R\left(A + B\frac{T}{100} + D\frac{T^2}{100^2} \right) \tag{9}$$

$$v_{IL} = \left(\sum_{i=0}^{2} \left(D_i \left(T - 298.15 \right)^i \right) \right) + n\left(\sum_{i=0}^{2} \left(E_i \left(T - 298.15 \right)^i \right) \right) + \sum_{i=0}^{2} \left(F_i \left(T - 298.15 \right)^i \right) \tag{10}$$

3 Model and validation of absorption refrigeration cycle

To evaluate the thermodynamic performance of the selected HFO/[DCA] working pairs, both the conventional single-effect absorption refrigeration cycle and the compression-assisted absorption refrigeration cycle were considered. In the single-effect cycle, the low-pressure refrigerant vapor generated in the evaporator is absorbed by the refrigerant-lean ionic-liquid solution in the absorber, releasing absorption heat and forming a refrigerant-rich solution. The rich solution is then pressurized by the solution pump and preheated in the solution heat exchanger before entering the generator, where external heat is supplied to desorb the refrigerant from the solution. The released high-pressure refrigerant vapor flows into the condenser, rejects heat and condenses into liquid refrigerant, which is subsequently throttled through the refrigerant expansion valve and returns to the evaporator to produce the cooling effect. Meanwhile, the refrigerant-lean solution leaving the generator is cooled in the solution heat exchanger, depressurized through the solution valve and returned to the absorber, thereby completing the solution circulation loop[16-18]. Compared with the single-effect configuration, the compression-assisted cycle introduces a refrigerant compressor between the evaporator and absorber. The refrigerant vapor from the evaporator is compressed to a higher absorption pressure before entering the absorber, which enhances the absorption driving force, increases the concentration difference between the rich and lean solutions, and reduces the required solution circulation ratio. Therefore, the compression-assisted configuration can improve the adaptability of the absorption refrigeration cycle to low-grade heat sources, although additional compressor work is required[19,20]. The basic configurations of the two cycles are shown in Figs. 1 and 2.

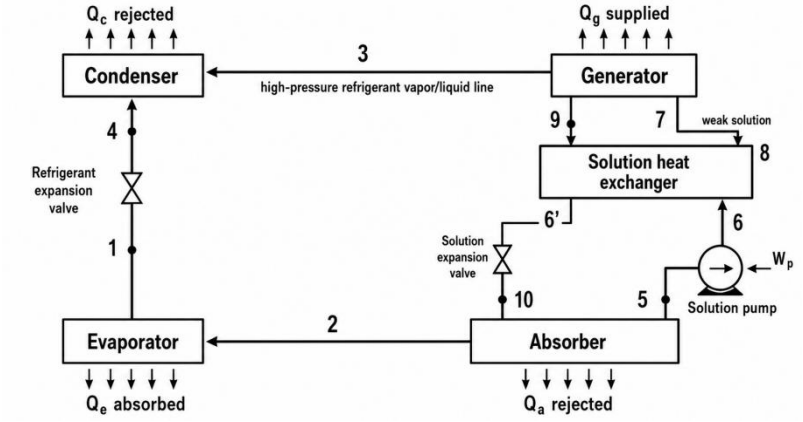


Fig. 1 Schematic diagram of the absorption refrigeration cycle

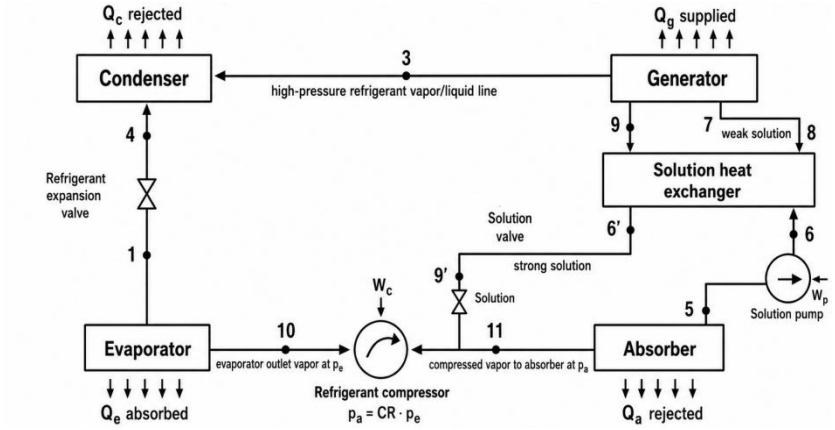


Fig. 2 Schematic diagram of the compression-assisted absorption refrigeration cycle

To investigate the cycle performance of the selected HFO/[DCA] working pairs, a thermodynamic model of the absorption refrigeration cycle was established based on the component mass and energy balances. The model was applied to both the conventional single-effect absorption refrigeration cycle and the compression-assisted absorption refrigeration cycle. In the model, the HFO refrigerant was treated as the volatile component, while the ionic liquid was regarded as a non-volatile absorbent. The vapor-liquid equilibrium relationship obtained from the NRTL model was used to determine the solution concentrations at the absorber and generator outlets.

For model simplification, several assumptions were introduced. The whole cycle was considered to operate under steady-state conditions. The refrigerant at the evaporator outlet and condenser outlet was assumed to be in a saturated state. The solutions leaving the absorber and generator were assumed to reach phase equilibrium at the corresponding temperatures and pressures. Pressure drops in pipelines and heat exchangers, flow resistance, heat loss to the surroundings, and changes in kinetic and potential energies were neglected. The throttling processes in the refrigerant expansion valve and solution expansion valve were assumed to be isenthalpic. The effectiveness of the solution heat exchanger was set to 80%. Since the work input of the solution pump is much smaller than the heat

transfer rates of the generator, absorber, condenser and evaporator, the pump work was neglected in the single-effect cycle calculation[21-23]. For the compression-assisted configuration, however, the refrigerant compressor work was included because it directly affects the system energy input and cycle performance.

Based on the conservation of mass and energy, the heat load of the generator can be calculated using Eq (11). In this equation, Qg represents the heat supplied to the generator, h_i denotes the specific enthalpy at state point i, m_w is the mass flow rate of the weak solution, and m_r is the mass flow rate of the refrigerant. In this work, the weak solution refers to the refrigerant-rich solution leaving the absorber, while the strong solution refers to the refrigerant-lean solution leaving the generator.

$$Q_g + m_r h_7 = m_r h_3 + (m_w - m_r) h_8 \quad (11)$$

The heat transfer rates of the absorber, condenser, evaporator and solution heat exchanger are calculated using Eqs. (12) – (15), respectively. In these equations, Qa, Qc, Qe and Qx denote the heat loads of the absorber, condenser, evaporator and solution heat exchanger, respectively. The enthalpy of each state point was obtained from the thermodynamic property model of the refrigerant/ionic-liquid solution. The heat exchanger was modeled using a fixed effectiveness, and the outlet temperatures of the solution streams were determined according to the heat balance and the specified heat-exchanger effectiveness.

$$Q_a + m_w h_5 = m_r h_{11} + (m_w - m_r) h_{10} \quad (12)$$

$$Q_a + m_w h_5 = m_r h_{11} + (m_w - m_r) h_{10} \quad (13)$$

$$Q_c + m_r h_4 = m_r h_3 \quad (14)$$

$$Q_e + m_r h_1 = m_r h_2 \quad (15)$$

$$Q_x = (m_w - m_r)(h_8 - h_9) \quad (16)$$

The circulation ratio is an important indicator for evaluating the matching performance of refrigerant/ionic-liquid working pairs in absorption refrigeration cycles. It reflects the amount of solution that must be circulated to produce a unit mass flow rate of refrigerant vapor. A lower circulation ratio generally indicates a smaller solution flow rate, lower heat load in the generator and absorber, and better cycle performance. The circulation ratio is defined by Eq. (16)[24,25], where m_s is the mass flow rate of the strong solution and x_w and x_s are the refrigerant mass fractions in the weak and strong solutions, respectively.

$$f = m_s / m_r = \frac{1 - X_w}{X_s - X_W} \quad (16)$$

The solution concentration difference is calculated using Eq. (17). This parameter directly reflects the absorption and desorption capacity of the working pair between the absorber and generator. A larger concentration difference is favorable for reducing the required solution circulation rate and improving the thermodynamic performance of the system.

$$W_C = \frac{m_r h_{11,i} - h_2}{\eta_i} = m_r(h_{11} - h_2) \tag{17}$$

For the single-effect absorption refrigeration cycle, the coefficient of performance is defined as the ratio of the cooling capacity produced in the evaporator to the heat input supplied to the generator, as shown in Eq. (18). For the compression-assisted cycle, the refrigerant vapor leaving the evaporator is compressed before entering the absorber. Therefore, the compressor work should be included in the total energy input when calculating the COP of the compression-assisted configuration. This treatment enables a consistent comparison between the single-effect and compression-assisted cycles under different operating conditions.

$$C_{\text{cop}} = \frac{Q_{\text{e}}}{Q_{\text{g}} + W_{\text{p}}} \tag{18}$$

$$C_{\text{cop}} = \frac{Q_{\text{e}}}{Q_{\text{g}} + W_{\text{c}}} \tag{19}$$

Where the W_c presents the efficiency of compressor in the refrigeration cycle.

2.1 Validation of Model Accuracy

To verify the reliability of the thermodynamic model and the calculation procedure, the absorption refrigeration cycle reported in the literature for the R1234ze(E)/[Emim][BF_4] working pair was recalculated under the same operating conditions[26]. The predicted cycle performance was then compared with the published data. As shown in Fig. 3, the model results agree well with the literature values over the investigated range of generator outlet temperatures, where the absorber and condenser temperatures were both fixed at 35℃ and the evaporator temperature was set to 5℃. The small deviations between the present results and the reference data may be attributed to differences in the iterative solution strategy. Therefore suitable for the subsequent performance analysis of the four HFO/[DCA] working pairs.

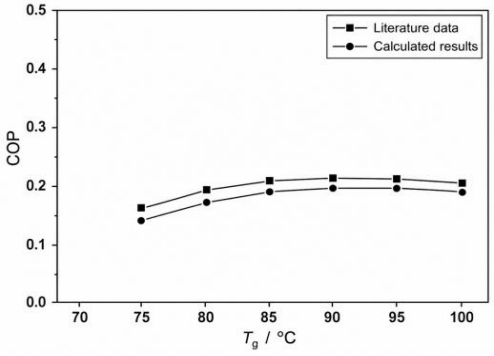


Fig.3 Validation the performances between the working pair of R1234ze(E) and [Emim][BF4] in the hybrid system

3. Results and Discussion

To evaluate the applicability of the selected HFO/[DCA] working pairs in absorption

refrigeration systems, a comparative thermodynamic analysis was performed for R1234yf/[C_2mim][DCA], R1234yf/[C_4mim][DCA], R1234ze(E)/[C_2mim][DCA] and R1234ze(E)/[C_4mim][DCA]. The effects of generator temperature, condenser temperature, absorber temperature and evaporator temperature on the circulation ratio, solution concentration difference, COP and exergy efficiency were systematically examined. In addition, the performance variation between the conventional single-effect cycle and the compression-assisted absorption refrigeration cycle was further analyzed to clarify the influence of absorption-pressure enhancement on the four working pairs.

3.1 Effects of generator temperature and condenser temperature on system performance

The circulation ratios of four ionic-liquid working pairs were compared in both the single-effect absorption refrigeration cycle and the compression-assisted absorption refrigeration cycle. Fig.4 and Fig.5 presents the variation of the circulation ratio with generator temperature. The evaporator, condenser, and absorber temperatures were set to 5°C, 35°C, and 30°C, respectively.

The results show that the circulation ratio decreases continuously as the generator temperature increases. This is mainly because a higher generator temperature promotes refrigerant desorption from the ionic-liquid solution and increases the concentration difference between the refrigerant-rich and refrigerant-lean solutions. Compared with the single-effect cycle, the compression-assisted cycle exhibits a much lower circulation ratio under the same generator temperature,even in the low generator temperature. Among the four investigated working pairs, R1234ze(E)/[C_4mim][DCA] shows the lowest circulation ratio, followed by R1234ze(E)/[C_2mim][DCA], R1234yf/[C_4mim][DCA] and R1234yf/[C_2mim][DCA]. This trend suggests that R1234ze(E)-based working pairs, especially R1234ze(E)/[C_4mim][DCA], are more favorable for absorption refrigeration applications under the investigated operating conditions. It should be noted that the R1234yf-based systems are not evaluated at 100 °C, because this generator temperature is close to or exceeds the applicable saturation-property range near the critical temperature of R1234yf.

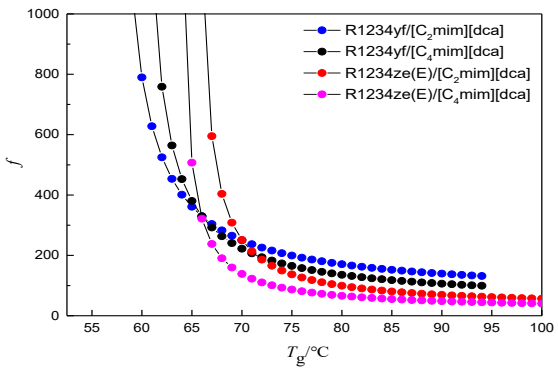


Fig. 4 Effect of generator temperature on the circulation ratio of the single-effect system

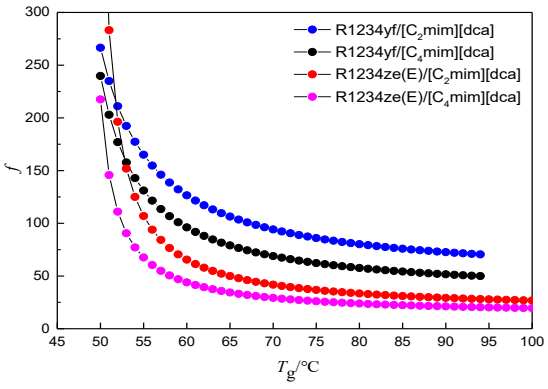


Fig. 5 Effect of generator temperature on the circulation ratio of the compression-assisted cycle

The condenser temperature is an important operating parameter affecting the high-pressure side of the absorption refrigeration cycle. A lower condenser temperature is beneficial to cycle

performance because it reduces the condensation pressure and facilitates refrigerant desorption in the generator.

As shown in Fig.6 and Fig.7, the circulation ratio increases continuously with increasing condenser temperature for all four HFO/[DCA] working pairs. When the condenser temperature decreases from 35℃to 30℃, the circulation ratio is reduced, indicating that a smaller solution flow rate is required to generate the same refrigerant mass flow rate. In contrast, with the increase of condenser temperature the refrigerant saturation pressure on the high-pressure side of the cycle. It is worth noting that the circulation ratio of R1234ze(E)/[C_2mim][DCA] increases sharply at higher condenser temperatures in the single-effect cycle. This abrupt increase is mainly attributed to the rapid reduction in the available solution concentration difference when the condenser pressure approaches the upper operating limit of the working pair.

Among the four working pairs, R1234ze(E)/[C_4mim][DCA] consistently exhibits the lowest circulation ratio as the condenser temperature increases from 30℃ to 55℃. This results indicates that R1234ze(E)/[C_4mim][DCA] requires the lowest solution circulation flow rate under the same operating conditions and therefore shows the most favorable thermodynamic matching characteristics. Moreover, the increase in circulation ratio becomes more pronounced at higher condenser temperatures, suggesting that the cycle becomes more sensitive to condensation pressure when the concentration lift approaches its operating limitation. Therefore, an excessively high condenser temperature should be avoided in practical absorption refrigeration operation, especially for working pairs with relatively small concentration differences.

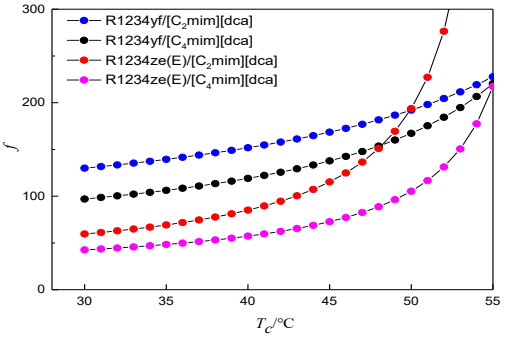


Fig.6 Effect of circulation ratio under different condenser temperatures in single-effect cycle

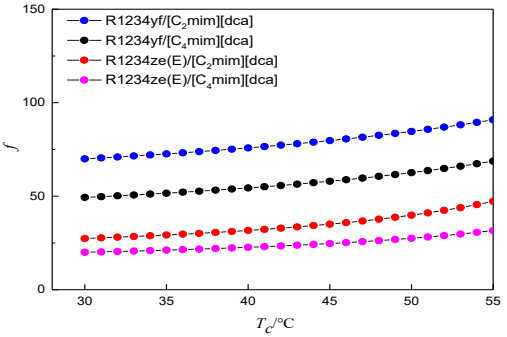


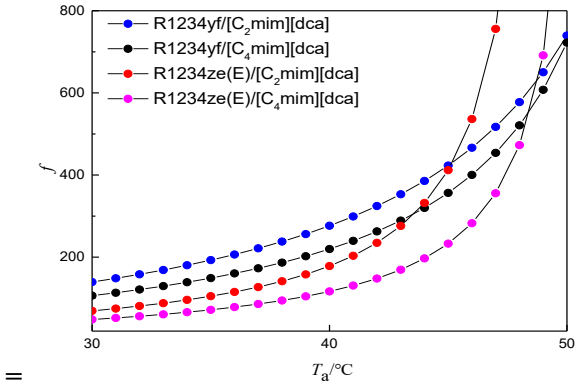
Fig.7 Effect of circulation ratio under different condenser temperatures in compression-assisted cycle

3.2 Effect of absorber temperature on system performance

As shown in Fig.8 and Fig.9, with the absorber temperature increases, the refrigerant concentration in the refrigerant-rich solution decreases, which reduces the concentration difference between the refrigerant-rich and refrigerant-lean solutions. Consequently, a larger solution circulation flow rate is required to produce the same refrigerant mass flow rate. Among the four working pairs, R1234ze(E)/[C_4mim][DCA] consistently exhibits the lowest circulation ratio, followed by

R1234ze(E)/[C2mim][DCA], R1234yf/[C4mim][DCA] and R1234yf/[C2mim][DCA].

Compared with the conventional single-effect cycle, the compression-assisted cycle shows lower circulation ratios at the same absorber temperature because the increased absorption pressure enhances refrigerant solubility in the ionic-liquid solution. However, both cycles exhibit the same increasing trend with absorber temperature, indicating that excessive absorber temperature is unfavorable to refrigerant absorption and should be avoided in practical operation. Therefore, lowering the absorber temperature is beneficial for improving the absorption capacity, reducing the solution circulation requirement and enhancing the overall cycle performance.



=

Fig.8 Variation in system performance with absorber temperature in single-effect cycle

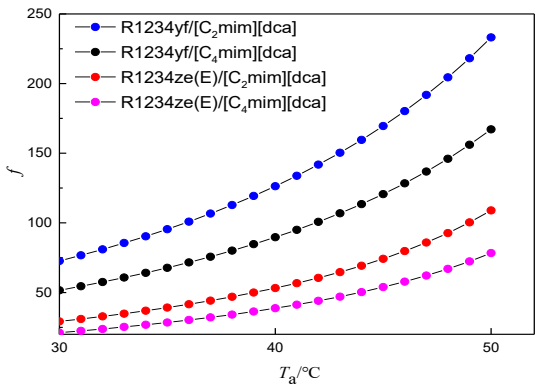


Fig.9 Variation in system performance with absorber temperature in compression-assisted cycle

3.3 Effect of evaporator temperature on system performance

The evaporator temperature determines the evaporating pressure and directly affects refrigerant absorption in the ionic-liquid solution. To evaluate this effect, the circulation ratios of the four working pairs were calculated at generator temperature of 90 °C and absorber temperature of 30 °C, with condenser temperatures of 30 °C and 35 °C, as shown in Fig 6 and Fig7. The results show that the circulation ratio decreases continuously with increasing evaporator temperature within the feasible operating range. This is mainly because a higher evaporator temperature increases the evaporating pressure, enhances refrigerant absorption in the absorber and enlarges the concentration difference between the refrigerant-rich and refrigerant-lean solutions.

At a condenser temperature of 30 °C, increasing the evaporator temperature from 5 °C to 35 °C reduces the circulation ratio of R1234ze(E)/[C4mim][DCA] from 48.32 to 8.09, while that of R1234yf/[C2mim][DCA] decreases from 139.43 to 37.08. A similar trend is observed at a condenser temperature of 35 °C, although the circulation ratios are higher because of the increased high-pressure-side saturation pressure. Among the four working pairs, R1234ze(E)/[C4mim][DCA] consistently exhibits the lowest circulation ratio, followed by R1234ze(E)/[C2mim][DCA], R1234yf/[C4mim][DCA] and R1234yf/[C2mim][DCA]. Compared with the single-effect cycle, the compression-assisted cycle shows lower circulation ratios at the same evaporator temperature, indicating that absorption-pressure enhancement can improve refrigerant solubility and reduce the

required solution flow rate. However, when the evaporator temperature approaches the absorber or condenser temperature, the pressure hierarchy and heat-transfer driving force of the cycle may no longer be maintained. Therefore, increasing the evaporator temperature is beneficial only within the feasible operating range.

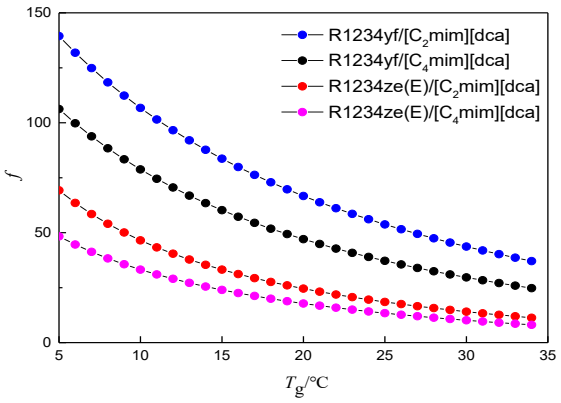


Fig.10 Effect of evaporator temperature on the circulation ratio of working pairs in single-effect cycle

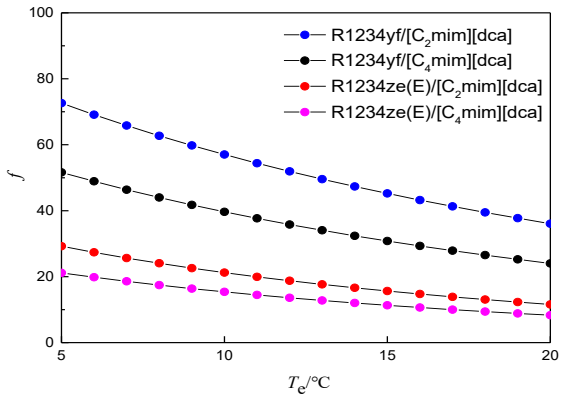


Fig.11 Effect of evaporator temperature on the circulation ratio of working pairs in compression-assisted cycle

4.4 Effect of solution concentration difference on system performance

In absorption refrigeration cycles, the solution concentration difference reflects the refrigerant mass-fraction variation between the solution leaving the absorber and that generator. In this work, the refrigerant mass fraction in the refrigerant-rich solution leaving the absorber and the refrigerant-lean solution leaving the generator. This parameter directly determines the required solution circulation rate. A larger concentration difference indicates that more refrigerant can be desorbed per unit mass flow rate of solution, thereby reducing the circulation ratio and improving the cycle performance. As shown in Fig 12, the solution concentration difference increases with the generator temperature for all the working pairs. This is because a higher generator temperature enhances refrigerant desorption in the generator and decreases the refrigerant concentration in the lean solution, leading to a larger concentration lift between the absorber and generator. In the single-effect cycle, the concentration difference of R1234ze(E)/[C4mim][DCA] increases Sharply while the temperature increases from 63℃ to 90℃ temperature range. For the R1234yf-based working pairs, the concentration difference also increases with generator temperature but remains relatively smaller. R1234yf/[C2mim][DCA] increases from 0.019 percentage points at 55 °C to 0.71 percentage points at 90 °C. The data at 100 °C are not considered for the R1234yf-based systems because this temperature exceeds the applicable saturation-property range near the critical temperature of R1234yf.

Compared with the conventional single-effect cycle, the compression-assisted cycle produces a significantly larger concentration difference at the same generator temperature. At 90°C, the concentration difference of R1234ze(E)/[C4mim][DCA] increases from 0.43 percentage points in the single-effect cycle to 5.04 percentage points in the compression-assisted cycle. Similarly, the

concentration differences of R1234ze(E)/[C2mim][DCA], R1234yf/[C2mim][DCA] and R1234yf/[C4mim][DCA] increase from 0.36, 0.18 and 0.43 percentage points to 1.41, 3.68 and 5.04 percentage points, respectively. This improvement is mainly attributed to the increased absorption pressure, which enhances refrigerant solubility in the ionic-liquid absorbent and increases the refrigerant concentration of the rich solution.

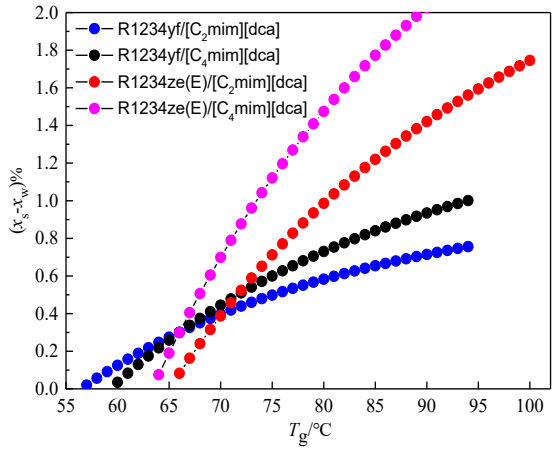


Fig.12 Effect of generator temperature on the solution concentration difference in single-effect cycle

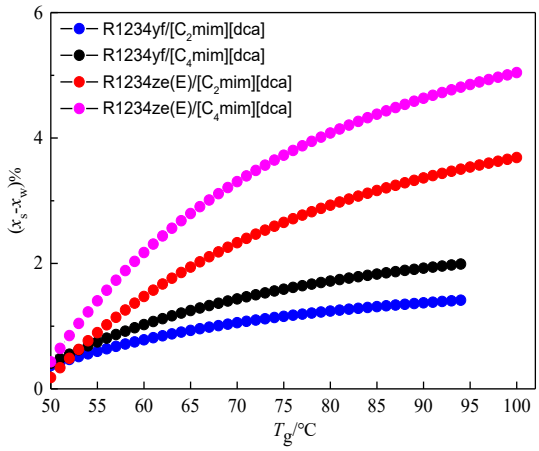


Fig.13 Effect of generator temperature on the solution concentration difference in the compression-assisted cycle

Overall, R1234ze(E)/[C4mim][DCA] exhibits the largest solution concentration difference among the four working pairs, followed by R1234ze(E)/[C4mim][DCA]＞R1234ze(E)/[C2mim][DCA]＞R1234yf/[C4mim][DCA]＞R1234yf/[C2mim][DCA]. This order is consistent with the circulation-ratio results, confirming that the solution concentration difference is the key factor governing the solution circulation requirement. The larger concentration difference of R1234ze(E)/[C4mim][DCA] explains its lower circulation ratio and more favorable refrigeration-cycle performance under the investigated operating conditions.

4.5 COP and exergy efficiency of different working pairs

In absorption refrigeration cycles, the coefficient of performance (COP) is one of the most important indicators for evaluating the overall thermodynamic performance of working pairs. In this study, the COP values of four HFO/[DCA] working pairs were calculated and compared for both the conventional single-effect absorption refrigeration cycle and the compression-assisted absorption refrigeration cycle. As shown in Fig. 14 and Fig 15, the COP of the working pairs generally increases with the increasing of generator temperature.

For the single-effect absorption refrigeration cycle, the value of COP at lower generator temperatures is mainly attributed to enhanced refrigerant desorption in the generator. A higher generator temperature increases the concentration difference between the refrigerant-rich and refrigerant-lean solutions, thereby reducing the solution circulation ratio and improving the cooling

performance. However, when the generator temperature continues to increase, the improvement in solution concentration difference becomes less significant, whereas the generator heat input still increases. As a result, the growth rate of COP gradually decreases, and the COP may even decline slightly at higher generator temperatures. For the compression-assisted absorption refrigeration cycle, the refrigerant vapor from the evaporator is compressed before entering the absorber. This increases the absorption pressure, improves refrigerant solubility in the ionic-liquid absorbent and enlarges the concentration difference between the refrigerant-rich and refrigerant-lean solutions. Consequently, the compression-assisted cycle shows a lower circulation ratio and better adaptability to low-grade heat-source conditions than the single-effect cycle. In terms of COP, the compression-assisted configuration can improve the cycle performance when the reduction in generator heat input and solution circulation requirement outweighs the additional compressor work. However, because the compressor work becomes an extra energy input, the COP improvement is not simply proportional to the increase in absorption pressure. Therefore, the compression-assisted cycle should be evaluated by considering both the enhanced absorption effect and the additional power consumption.

Among the four working pairs, R1234ze(E)/[C4mim][DCA] shows the most favorable coefficient of performance, followed by R1234ze(E)/[C2mim][DCA] ＞ R1234yf/[C4mim][DCA] ＞ R1234yf/[C2mim][DCA]. For R1234ze(E)/[C4mim][DCA], the COP values reaches a maximum value of 0.11 at a generator temperature of 90°C. Overall, the compression-assisted cycle is more advantageous for improving the operating feasibility of HFO/[DCA] working pairs under relatively low generator temperatures, while the single-effect cycle remains simpler and avoids additional mechanical work input.

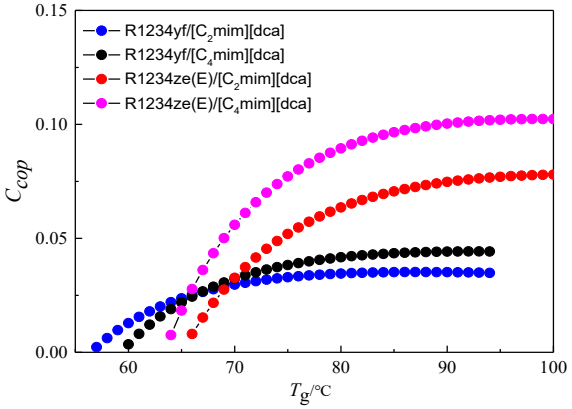


Fig.14 Performance of different working pairs in single-effect cycle.

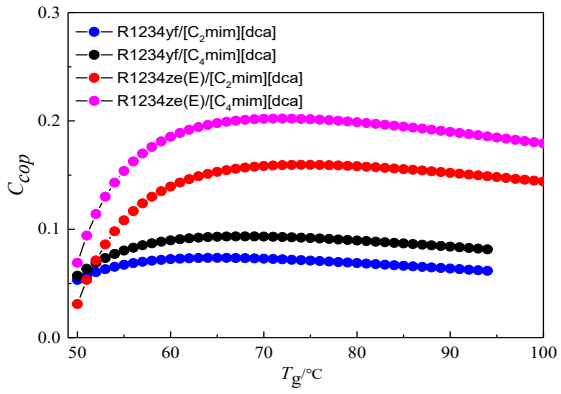


Fig.15 Performance of different working pairs in compression-assisted cycle

To further evaluate the exergy efficiency of the four working pairs in the single-effect absorption refrigeration cycle and compression-assisted cycle were also calculated, and its variation with generator temperature was analyzed. The exergy efficiency is expressed as

$$\eta_{Ex}=\frac{E_{Q_e}}{E_{Q_g}}=C_{COP}\frac{\left|1-T_{ref}/T_e\right|}{\left(1-T_{ref}/T_g\right)} \tag{19}$$

where E_{Q_e} and E_{Q_g} represents the exergy ； T_{ea} *and* T_g are the evaporator and generator temperatures; T_{ref} is set to 298.15 K[27-30].

Figure.16 and Figure.17 shows the system at a condenser temperature of 35 °C and absorber temperature of 35 °C, and an evaporator temperature of 5 °C. The results indicate that the system exergy efficiency first increases and then decreases slowly as the generator temperature rises. Comparison of the working pairs shows that the exergy efficiency of R1234ze(E)/[C_4mim][DCA] has reached 0.051 at the generator temperature of 80°C in single effect cycle , the maximum exergy efficiencies of are 0.165 at the generator temperature of 58°C in the compression-assisted cycle.

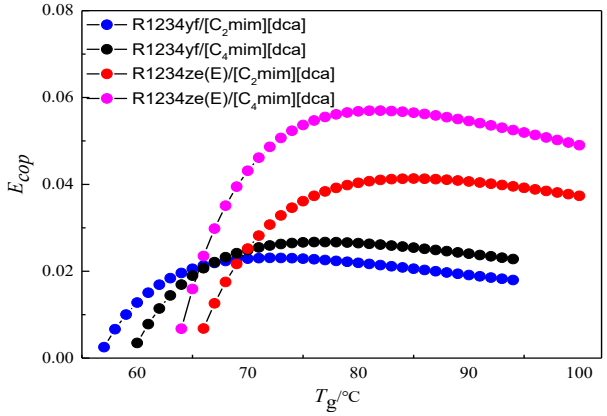


Fig. 16 Exergy efficiency for the four working pairs in single cycle

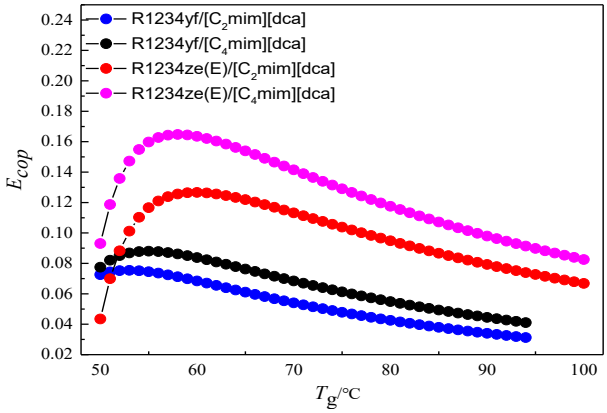


Fig. 17 Exergy efficiency for the four working pairs in compression-assisted cycle

5. Conclusions

Among the four investigated working pairs, shows that the generator temperature has a significant influence on the cycle performance. Increasing the generator temperature enhances refrigerant desorption, enlarges the concentration difference between the refrigerant-rich and refrigerant-lean solutions, and reduces the circulation ratio. However, when the generator temperature becomes sufficiently high, the improvement in concentration difference gradually weakens, and the COP tends to level off or decrease slightly. Increasing the evaporator temperature is beneficial to cycle performance within the feasible operating range because it increases the evaporating pressure and enhances refrigerant absorption. In contrast, higher condenser and absorber temperatures reduce the available concentration difference and increase the circulation ratio, leading to performance deterioration.

Compared with the conventional single-effect cycle, the compression-assisted absorption refrigeration cycle presents lower circulation ratios and larger solution concentration differences under the same operating conditions. This is mainly because the increased absorption pressure improves

refrigerant solubility in the ionic-liquid absorbent and strengthens the absorption process. The overall performance follows the order R1234ze(E)/[C_4mim][DCA]>R1234ze(E)/[C_2mim][DCA]> R1234yf/[C_4mim][DCA]>R1234yf/[C_2mim][DCA]. This result indicates that R1234ze(E)-based working pairs are more suitable for ionic-liquid-based absorption refrigeration applications than R1234yf-based systems under the investigated conditions. Results provide theoretical guidance for selecting low-GWP refrigerant/ionic-liquid working pairs and optimizing single-effect and compression-assisted absorption refrigeration cycles.

Funding : This work was supported by the Joint Fund of Henan Provincial Science and Technology Research and Development Program (No.252103810078). Key Scientific Research Project of Henan Provincial Department of Education (No. 24A470003): Development and Key Technology Research of Ionic Liquid-Based Absorption Refrigeration Working Pairs for Solar Refrigeration and Air Conditioning.

Data availability

The data supporting the findings of this study are available from the corresponding author upon reasonable request.

References

[1] Ji L, Shukla S K, Zuo Z, Lu X, Ji X, Wang C. An overview of the progress of new working pairs in absorption heat pumps. Energy Reports, 2023, 9: 703–729.

[2] Kim Y J, Kim S, Joshi Y K, Fedorov A G, Kohl P A. Thermodynamic analysis of an absorption refrigeration system with ionic-liquid/refrigerant mixture as a working fluid. Energy, 2012, 44(1): 1005–1016.

[3] Kallitsis K, Koulocheris V, Pappa G, Voutsas E. Evaluation of water + imidazolium ionic liquids as working pairs in absorption refrigeration cycles. Applied Thermal Engineering, 2023, 233: 121201.

[4] Chu J, Zhang Z, Liu X, He M. Estimating the solubility of HFC/HFO in ionic liquids from molecular structure using machine learning method. Chemical Engineering Research and Design, 2022, 184: 315–325.

[5] Liu X, Bai L, Liu S, He M. Vapor–liquid equilibrium of R1234yf/[HMIM][Tf_2N] and R1234ze(E)/[HMIM][Tf_2N] working pairs for the absorption refrigeration cycle. Journal of Chemical & Engineering Data, 2016, 61(11): 3952–3957.

[6] Asensio-Delgado S, Viar M, Pardo F, Zarca G, Urtiaga A. Gas solubility and diffusivity of hydrofluorocarbons and hydrofluoroolefins in cyanide-based ionic liquids for the separation of refrigerant mixtures. Fluid Phase Equilibria, 2021, 549: 113210.

[7] Renon H, Prausnitz J M. Local compositions in thermodynamic excess functions for liquid mixtures. AIChE Journal, 1968, 14(1): 135–144.

[8] Lemmon E W, Bell I H, Huber M L, McLinden M O. NIST Standard Reference Database 23: Reference Fluid Thermodynamic and Transport Properties—REFPROP, Version 10.0. National Institute of Standards and Technology, Standard Reference Data Program, Gaithersburg, 2018.

[9] Shiflett M B, Harmer M A, Junk C P, Yokozeki A. Solubility and diffusivity of difluoromethane in

room-temperature ionic liquids. Journal of Chemical & Engineering Data, 2006, 51(2): 483–495.

[10] Shiflett M B, Yokozeki A. Solubilities and diffusivities of hydrofluorocarbons in room-temperature ionic liquids. AIChE Journal, 2006, 52(3): 1205–1219.

[11] Wu W, Zhang H, You T, Li X. Thermodynamic investigation and comparison of absorption cycles using hydrofluoroolefins and ionic liquid. Industrial & Engineering Chemistry Research, 2017, 56(35): 9906–9916.

[12] Sun Y, Zhang Y, Di G, Wang X, Prausnitz J M, Jin L. Vapor–liquid equilibria for R1234ze(E) and three imidazolium-based ionic liquids as working pairs in absorption–refrigeration cycle. Journal of Chemical & Engineering Data, 2018, 63(8): 3053–3060.

[13] Asensio-Delgado J M, Asensio-Delgado S, Zarca G, Urtiaga A. Analysis of hybrid compression absorption refrigeration using low-GWP HFC or HFO/ionic liquid working pairs. International Journal of Refrigeration, 2022, 134: 232–241.

[14] Sun Y, Di G, Wang J, Wang X, Wu W. Performance analysis of R1234yf/ionic liquid working fluids for single-effect and compression-assisted absorption refrigeration systems. International Journal of Refrigeration, 2020, 109: 25–36.

[15] Kim S, Kohl P A. Theoretical and experimental investigation of an absorption refrigeration system using R134a/[bmim][PF_6] working fluid. Industrial & Engineering Chemistry Research, 2013, 52(38): 13459–13465.

[16] Kim S, Kohl P A. Analysis of [hmim][PF_6] and [hmim][Tf_2N] ionic liquids as absorbents for an absorption refrigeration system. International Journal of Refrigeration, 2014, 48: 105–113.

[17] Wang M, Becker T M, Infante Ferreira C A. Assessment of vapor–liquid equilibrium models for ionic-liquid-based working pairs in absorption cycles. International Journal of Refrigeration, 2018, 87: 10–25.

[18] Moreno D, Ferro V R, de Riva J, Santiago R, Moya C, Larriba M, Palomar J. Absorption refrigeration cycles based on ionic liquids: Refrigerant/absorbent selection by thermodynamic and process analysis. Applied Energy, 2018, 213: 179–194.

[19] Qian Z, Xu C, Ren J. Thermal analysis of a novel single-effect absorption refrigeration system using water/ionic liquid as working fluids. Thermal Science, 2022, 26(4A): 3107–3118.

[20] Ayou D S, Coronas A. Performance analysis of absorption heat transformer cycles using ionic liquids based on imidazolium cation as absorbents with 2,2,2-trifluoroethanol as refrigerant. Energy Conversion and Management, 2014, 84: 512–523.

[21] Li X, Xu S, Li J. Absorption refrigeration cycle driven by waste heat using R124/DMAC as working fluids. Journal of Chemical Industry and Engineering, 2015, 66(5): 1883–1890.

[22] Wu W, You T, Zhang H, Li X. Comparisons of different ionic liquids combined with trans-1,3,3,3-tetrafluoropropene (R1234ze(E)) as absorption working fluids. International Journal of Refrigeration, 2018, 88: 45–47.

[23] Kim Y J, Gonzalez M. Exergy analysis of an ionic-liquid absorption refrigeration system utilizing waste heat from data centers. International Journal of Refrigeration, 2014, 48: 26–37.

[24] [24] Wang M, Becker T M, Infante Ferreira C A. Assessment of vapor–liquid equilibrium models for ionic-liquid-based working pairs in absorption cycles. International Journal of Refrigeration, 2018, 87: 10–25.

[25] Moreno D, Ferro V R, de Riva J, Santiago R, Moya C, Larriba M, Palomar J. Absorption refrigeration cycles based on ionic liquids: Refrigerant/absorbent selection by thermodynamic and process analysis. Applied Energy, 2018, 213: 179–194.
[26] Qian Z, Xu C, Ren J. Thermal analysis of a novel single-effect absorption refrigeration system using water/ionic liquid as working fluids. Thermal Science, 2022, 26(4A): 3107–3118.
[27] Ayou D S, Coronas A. Performance analysis of absorption heat transformer cycles using ionic liquids based on imidazolium cation as absorbents with 2,2,2-trifluoroethanol as refrigerant. Energy Conversion and Management, 2014, 84: 512–523.
[28] Lee Y, Chu C, Beom T, Kim S, Kim J, Kim D K. Performance analysis of double-effect absorption refrigeration systems using hydrofluoroolefin refrigerants and ionic liquid absorbents. Case Studies in Thermal Engineering, 2025, 70: 106141.
[29] Asensio-Delgado J M, Asensio-Delgado S, Zarca G, Urtiaga A. Analysis of hybrid compression absorption refrigeration using low-GWP HFC or HFO/ionic liquid working pairs. International Journal of Refrigeration, 2022, 134: 232–241.
[30] Sun Y, Di G, Wang J, Wang X, Wu W. Performance analysis of R1234yf/ionic liquid working fluids for single-effect and compression-assisted absorption refrigeration systems. International Journal of Refrigeration, 2020, 109: 25–36.